



# CHORUS

This is the accepted manuscript made available via CHORUS. The article has been published as:

## Role of vibrational and configurational excitations in stabilizing the $L1_{2}$ structure in Co-rich Co-Al-W alloys

Robert K. Rhein, Philip C. Dodge, Min-Hua Chen, Michael S. Titus, Tresa M. Pollock, and Anton Van der Ven

Phys. Rev. B **92**, 174117 — Published 23 November 2015

DOI: [10.1103/PhysRevB.92.174117](https://doi.org/10.1103/PhysRevB.92.174117)

# The Role of Vibrational and Configurational Excitations in Stabilizing the L1<sub>2</sub> Structure in Co-rich Co-Al-W Alloys

Robert K. Rhein, Philip C. Dodge, Min-Hua Chen, Michael S. Titus, Tresa M. Pollock, and Anton Van der Ven\*

*Materials Department, University of California Santa Barbara, Santa Barbara, CA 93106-5050, USA*

(Dated: November 4, 2015)

A first-principles study of the L1<sub>2</sub> Co<sub>3</sub>(Al,W) phase was performed to assess phase stability at elevated temperature. Configurational degrees of freedom were treated with a cluster expansion and Monte Carlo simulations while contributions to the free energy from vibrational excitations were determined within the quasi-harmonic approximation accounting for effects of thermal expansion. It was found that while contributions from configurational degrees of freedom are important, vibrational entropy is crucial in making L1<sub>2</sub> Co<sub>3</sub>(Al,W) stable at high temperature in the Co-rich portion of the Co-Al-W ternary. The emergence of L1<sub>2</sub> at high temperature can be attributed to a large difference in vibrational entropy between the close packed fcc based L1<sub>2</sub> phases and the energetically stable, yet vibrationally stiff B2 CoAl compound.

## I. INTRODUCTION

Ni-base superalloys are the current design standard for high-temperature turbine blades in aerospace and energy-generation engines due to the creep resistance provided by their two-phase microstructure at high temperature<sup>1</sup>. The discovery of Co-Al-W alloys exhibiting a morphologically-identical microstructure in 2006 by Sato, et al. has opened the possibility of developing Co-base alloys with better creep resistance due to the higher melting temperature of Co relative to Ni<sup>2,3</sup>. Like their Ni-base counterparts, these Co-base alloys possess a two-phase microstructure of coherent, cuboidal  $\gamma'$  L1<sub>2</sub> precipitates embedded within a  $\gamma$  fcc solid solution matrix. In the Co<sub>3</sub>(Al,W) L1<sub>2</sub> phase, Co occupies face centered sites (A sublattice) and Al and W occupy the face corner sites (B sublattice)<sup>4</sup>. The coherent  $\gamma'$  L1<sub>2</sub> precipitates are responsible for the increased resistance to plastic deformation at elevated temperature in Co-base superalloys, resulting in a similar positive flow stress anomaly as Ni-base superalloys<sup>5,6</sup>. Because of this strengthening effect, the thermodynamic stability of the L1<sub>2</sub> phase at elevated temperature is a critical design parameter and has been examined both by using experiments and computational methods.

Initial experimental evidence indicated that L1<sub>2</sub> is a stable phase at 1173 K but exhibits metastability at 1273 K, decomposing into a three phase equilibrium of A1 Co, B2 CoAl and either D0<sub>19</sub> Co<sub>3</sub>W or D8<sub>5</sub> Co<sub>7</sub>W<sub>6</sub><sup>2,7</sup>. However, subsequent diffusion couple experiments suggested that the L1<sub>2</sub> phase is metastable at 1273 K<sup>8</sup>. Similar trends in which B2 CoAl, A1 Co, and D0<sub>19</sub> Co<sub>3</sub>W volume fraction increased at the expense of  $\gamma'$  were observed in bulk and melt-spun alloys<sup>9,10</sup>. Notably, the  $\gamma'$  phase did not completely dissolve upon aging in any of these experiments and the kinetics of dissolution were extraordinarily slow. Further experiments conducted using a number of Co-rich compositions in the Co-Al-W phase diagram did not detect the presence of any ternary intermetallic compounds on solidification, including L1<sub>2</sub><sup>11</sup>. Other investigations on Co-Al-W alloys annealed at 1173

K for 1000 h concluded that  $\gamma'$  is not a metastable phase at this temperature<sup>12</sup>.

The sum of experimental evidence clearly demonstrates that the stability of L1<sub>2</sub> Co<sub>3</sub>(Al,W) phase is highly dependent on composition and that the free energy of L1<sub>2</sub> differs only marginally from that of the competing three phase region. Variations in processing techniques, heat treatments, and alloy compositions could all account for the discrepancies regarding  $\gamma'$  stability. This has led to extensive research on higher-order alloying additions that will further stabilize the L1<sub>2</sub> phase. Nb, Ta, and Ti in particular have been shown to increase the  $\gamma'$  solvus temperature and DFT calculations have shown that a number of d-block transition metal alloying additions stabilize L1<sub>2</sub> relative to competing phases<sup>13-16</sup>.

Initial density functional theory calculations using the special quasi-random structure (SQS) approach with 32-atom supercells demonstrated that the 0 K formation energy of L1<sub>2</sub> Co<sub>3</sub>Al<sub>0.5</sub>W<sub>0.5</sub> is approximately 70 meV/atom less stable than a three phase mixture of B2 CoAl, A3 Co, and D0<sub>19</sub> Co<sub>3</sub>W<sup>17</sup>. The supercells considered in these calculations assumed equal mixing of Al and W on the B sublattice of the A<sub>3</sub>B L1<sub>2</sub> structure, although experimentally-observed compositions are off-stoichiometry with excess Co occupying B sites<sup>7</sup> and a W concentration that is higher than that of Al. Other DFT studies exploring the thermodynamic effects of adding vacancies and substitutional defects to the Co-Al-W L1<sub>2</sub> structure found that Co antisite defects on Al B-sites had a stabilizing effect<sup>18</sup>. Furthermore, finite temperature vibrational effects within the harmonic approximation at constant volume were found to increase L1<sub>2</sub> stability by reducing the free energy difference between L1<sub>2</sub> and the three-phase mixture from 70 meV/atom to 11 meV/atom at 1200 K. While this indicated a stabilizing effect due to vibrational contributions, it was not large enough to suggest that L1<sub>2</sub> is the most stable phase at 1200 K<sup>18</sup>.

In this work, we perform a first-principles investigation to establish the role of configurational and vibrational degrees of freedom in determining the stability of L1<sub>2</sub> relative to competing phases in the Co rich Co-Al-W alloys. We use the cluster expansion method combined

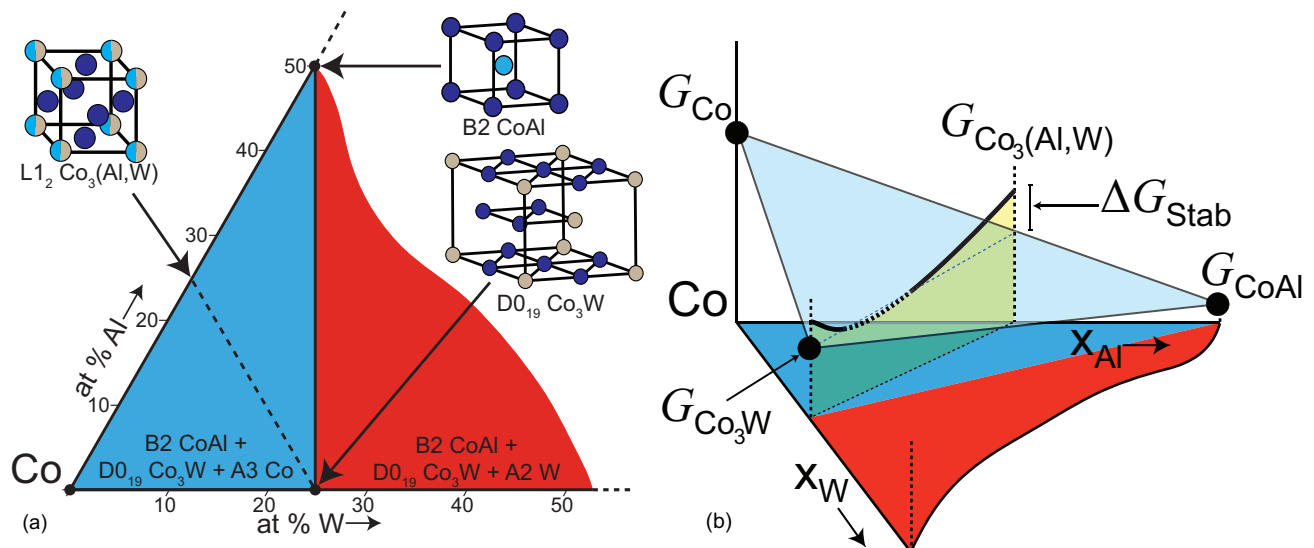


FIG. 1. (a) Co-rich part of the Co-Al-W phase diagram with labeled crystal structures. Regions with different 0 K ground states are labeled with different colors. Co undergoes a hcp to fcc transition at 723 K. The  $\text{Co}_3\text{Al}$ - $\text{Co}_3\text{W}$  pseudobinary line corresponding to the cluster expansion is shown. (b) Schematic of the free energies of the crystal structures in the Co-rich part of the Co-Al-W phase diagram at finite temperature.

with Monte Carlo simulations to calculate the configurational free energy of the  $\text{L}_{12}$  phase along the  $\text{Co}_3\text{Al}$ - $\text{Co}_3\text{W}$  pseudobinary line from first principles at elevated temperature. We also calculate vibrational free energies within the quasiharmonic approximation, thereby accounting for the effects of thermal expansion at high temperatures. We find that while configurational disorder over the B sublattice of  $\text{L}_{12}$  results in a sizable entropic contribution to the free energy, it is vibrational excitations that ultimately render the  $\text{L}_{12}$  phase stable at high temperature in the Co-Al-W ternary. The results of this study suggest that a lower bound for the temperature at which  $\text{L}_{12}$  becomes stable is 873 K.

## II. METHODOLOGY

Our goal was to assess the finite temperature stability of Co-rich  $\text{L}_{12}$  ordering in the Co-Al-W ternary system from first principles. Phase stability is determined by a global minimum of the Gibbs free energy, which can conveniently be visualized when plotting free energies as a function of atomic fractions as schematically illustrated in Figure 1. At low temperature, Co-rich alloys in the Co-Al-W ternary decompose into a three phase mixture consisting of pure Co, CoAl, and  $\text{Co}_3\text{W}$ . The free energy of this three phase mixture resides on a plane connecting the free energies of Co, CoAl and  $\text{Co}_3\text{W}$  as schematically shown in Figure 1. Pure Co is stable in the hcp crystal structure (A3) at low temperature, but transforms to fcc (A1) above 723 K while CoAl adopts the bcc-based B2 ordering.  $\text{Co}_3\text{W}$  is stable in the hcp-based  $\text{D}_{019}$  ordering. Although the experimentally observed  $\text{L}_{12}$  phase in the Co-Al-W system is Co rich, with excess Co oc-

cupying the Al and W sites, in this study we restricted ourselves to the pseudobinary  $\text{Co}_3\text{Al}_{1-x}\text{W}_x$  composition axis.  $\text{L}_{12}$  becomes thermodynamically stable at temperatures where the free energy of  $\text{Co}_3\text{Al}_{1-x}\text{W}_x$  drops below the plane connecting the free energies of Co, CoAl and  $\text{Co}_3\text{W}$ , as schematically illustrated in Figure 1.

Our analysis of phase stability incorporated the effects of both configurational and vibrational excitations. Configurational disorder due to W and Al mixing over the B sublattice of  $\text{L}_{12}$   $\text{A}_3\text{B}$  along the pseudobinary composition axis  $x$  in  $\text{L}_{12}$   $\text{Co}_3\text{Al}_{1-x}\text{W}_x$  will lead to important entropic contributions to the free energy at elevated temperature. Furthermore, several of the other phases that are stable at elevated temperature in the Co-rich part of the Co-Al-W composition space, including A1 Co, B2 CoAl, and  $\text{D}_{019}$   $\text{Co}_3\text{W}$ , may exhibit appreciable solid solubility. Prior experimental work and thermodynamic databases have established that the solid solubility of  $\text{D}_{019}$   $\text{Co}_3\text{W}$  is limited at elevated temperature<sup>2,19</sup> and it can therefore be approximated as a line compound. B2 CoAl, however, exhibits an appreciable degree of off stoichiometry as a result of Co antisite defects on the Al sublattice, analogous to B2 NiAl<sup>20,21</sup>. At 1173 K, the B2 structure can accommodate up to 33% Co on the Al sublattice<sup>2</sup>. The configurational entropy associated with this solid solubility may have a significant effect on the free energy of the B2 phase.

We accounted for contributions to the free energy arising from configurational disorder using the cluster expansion approach and Monte Carlo simulations. The Al and W ordering over the B sublattice of  $\text{L}_{12}$ , for example, can be described with occupation variables  $\sigma_i$  assigned to each site  $i$  of the B sublattice with each occupation variable taking values of +1 or -1 depending on whether

the site is occupied by Al or W. The collection of all occupation variables  $\vec{\sigma} = \{\sigma_1, \sigma_2, \dots, \sigma_N\}$  uniquely characterizes a configuration over  $N$  B-sublattice sites of  $L1_2$ . The formation energy,  $E(\vec{\sigma})$ , of a given configuration can then be expressed as an expansion in terms of polynomial basis functions according to:

$$E(\vec{\sigma}) = V_0 + \sum_{\alpha} V_{\alpha} \phi_{\alpha}(\vec{\sigma}) \quad (1)$$

where  $\phi_{\alpha}(\vec{\sigma})$  is a cluster function defined as the product of occupation variables belonging to the sites of a cluster labeled  $\alpha$ <sup>22</sup>. The coefficients of the cluster functions,  $V_{\alpha}$ , called effective cluster interactions (ECI), depend on the chemistry of the solid and are to be determined from first principles. The resultant cluster expansion can be rapidly evaluated in Monte Carlo simulations to calculate thermodynamic ensemble averages. The CASM package was used to construct and parameterize the cluster expansion and run the Monte Carlo simulations<sup>23–26</sup>.

We constructed binary cluster expansions for both  $L1_2$   $Co_3Al_{1-x}W_x$  and Co rich B2 CoAl due to the importance of configurational disorder in both phases. The expansion coefficients were fit to reproduce a training set of density functional theory energies, each corresponding to a particular ordering of W and Al over the B sublattice of  $L1_2$  or of Co and Al over the Al sublattice of B2 CoAl. A 4-atom  $L1_2$  primitive cell was used as a basis for supercell enumeration, in which the face corner site can be occupied by either Al or W, while the face center site is fixed to be Co. All symmetrically distinct configurations of Al and W over the B-sublattice in symmetrically distinct supercells ranging in size between one and five  $L1_2$  primitive cells were enumerated. Configurations on B2 supercells up to 18 atoms in size were enumerated from a 2-atom primitive cell in which the Al sublattice was allowed to vary between Al and Co.

The energies of the enumerated configurations as well as those of A1 and A3 Co and  $D0_{19}$   $Co_3W$  were calculated with density functional theory using the plane-wave pseudopotential based Vienna *Ab Initio* Simulation Package (VASP) code<sup>27,28</sup>. The Perdew, Burke, and Ernzerhof (PBE) generalized gradient approximation was used for the exchange and correlation functional with the projected augmented wave (PAW) pseudopotential method<sup>28–30</sup>. This functional was chosen because of its accuracy in calculating solid cohesive energies.<sup>31</sup> The energies of the ground state crystal structures and selected  $L1_2$  configurations were also calculated using the PBEsol functional<sup>32</sup>. An energy cutoff value of 400 eV and a gamma-centered k-point mesh were used. All calculations performed were spin-polarized. K-point convergence tests were performed to within an error of 0.5 meV/atom. Structures were initialized with lattice parameters corresponding to the experimentally-observed  $L1_2$   $Co_3(Al,W)$  3.57 Å and were subsequently fully relaxed.

We performed grand canonical Monte Carlo simulations on the cluster expansions to calculate the depen-

dence of chemical potential on concentration and temperature. A  $12 \times 12 \times 12$  simulation cell was used for  $L1_2$   $Co_3(Al_{1-x},W_x)$  in which B site occupancy was allowed to vary between Al and W. The free energy of  $L1_2$   $Co_3(Al_{1-x},W_x)$  was calculated by integrating the chemical potential with respect to  $x$  using  $Co_3Al$  as a reference. Monte Carlo simulations were also performed on the cluster expansion for B2 CoAl to calculate free energies using comparable parameters as for the  $L1_2$  structure.

Contributions from vibrational excitations were calculated within the quasi-harmonic approximation. We calculated vibrational free energies for both A1 and A3 Co and for the stoichiometric B2 CoAl and  $D0_{19}$   $Co_3W$  compounds. We estimated the vibrational free energy of  $L1_2$  along the pseudobinary composition axis  $Co_3(Al_{1-x},W_x)$  by linearly interpolating between the vibrational free energies of stoichiometric  $L1_2$   $Co_3Al$  and  $L1_2$   $Co_3W$ . Force constants were extracted from DFT calculations using the frozen phonon approach. Isolated atoms were displaced relative to their equilibrium positions in large supercells and the resultant forces on all atoms in the supercell were calculated using VASP. Force constants were obtained with a least-squares fit and used to construct the dynamical matrix to calculate phonon dispersion curves<sup>33</sup>. The volume of the supercells was allowed to vary  $\pm 5\%$  in 1% increments to enable the calculation of volume dependent Helmholtz free energies. A polynomial fit of the Helmholtz free energy as a function of volume was minimized to calculate the Gibbs free energy as a function of temperature at zero pressure.

### III. RESULTS

#### A. Ground State Energies and Pseudobinary Cluster Expansion

To parameterize a cluster expansion describing the dependence of the fully relaxed energy on configuration along the pseudobinary  $Co_3(Al_{1-x},W_x)$  composition axis, we calculated the energies of 63 symmetrically distinct Al and W orderings over the B sublattice of  $L1_2$ . The resulting formation energies  $\Delta E_f$  are shown in Fig. 2a. The formation energies were calculated according to:

$$\Delta E_f = E(\vec{\sigma}) - X_{Co}E_{Co} - X_{Al}E_{Al} - X_W E_W \quad (2)$$

in which  $E(\vec{\sigma})$  is the fully relaxed DFT total energy of configuration  $\vec{\sigma}$  and  $X_i$  and  $E_i$  represent the atomic fraction and DFT energy of the pure elements in their ground states using the PBE functional. Results obtained using the PBEsol functional yielded lattice parameters approximately 1% smaller but did not appreciably change the relative energies between crystal structures. Also shown in Fig. 2a is the energy of a three phase mixture of A3 Co-B2 CoAl- $D0_{19}$   $Co_3W$  evaluated along the pseudobinary composition axis  $x$ . Fig. 2a, clearly shows that  $L1_2$  along the pseudobinary composition axis is less stable

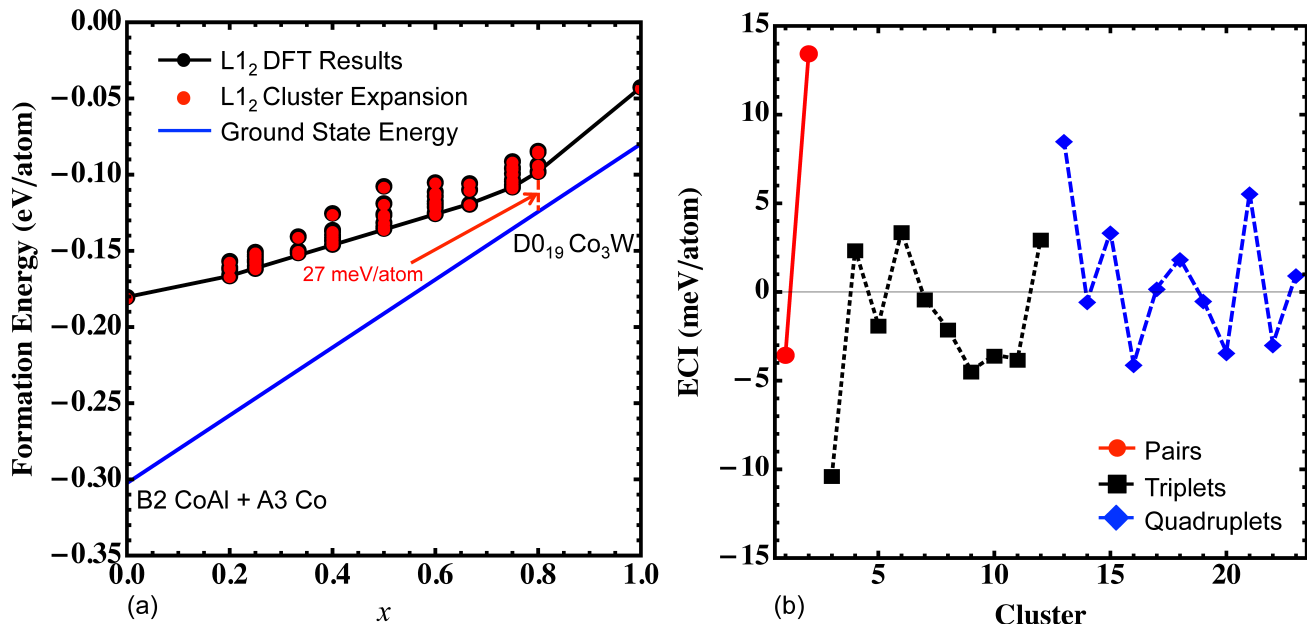


FIG. 2. (a) Ground state formation energies of the 63 L<sub>12</sub> configurations calculated via DFT and the cluster expansion results relative to the three-phase ground state.  $X_W$  represents the atomic fraction of W on the L<sub>12</sub> B sublattice. (b) Magnitude of effective cluster interaction versus cluster number for the L<sub>12</sub> structure.

than a three phase mixture comprising A3 Co-B2 CoAl-D0<sub>19</sub> Co<sub>3</sub>W.

The calculated formation energies in Fig. 2a indicate that many Al-W orderings over the B sublattice reside on the convex hull of metastable L<sub>12</sub>. Furthermore, the formation energies at fixed concentration  $x$  are all very close to each other, exhibiting only a weak dependence on configuration. This is likely due to the fact that the B sublattice sites are separated by a second nearest neighbor distance in fcc and screened by Co on the A sublattice. The variation of the formation energies with composition and configuration suggests that a solid solution due to Al-W disorder over the B sublattice should form at elevated temperatures in L<sub>12</sub> Co<sub>3</sub>(Al<sub>1-x</sub>W<sub>x</sub>).

At 0 K, there is no composition at which the L<sub>12</sub> crystal structure is favored relative to the three phase mixture, although it becomes more energetically competitive at compositions that are rich in W. The -605 meV/atom formation energy (relative to A3 Co and A1 Al) of B2 CoAl is the largest in magnitude of all structures considered, effectively destabilizing L<sub>12</sub> structures at the Al rich end of the pseudobinary. It is convenient to consider a relative stability free energy along the pseudobinary, defined as the difference between the free energy of a L<sub>12</sub> based configuration  $\vec{\sigma}$  at a particular concentration and the free energy of a three-phase mixture of Co, CoAl, and Co<sub>3</sub>W at the same composition:

$$\Delta G_{stab}(x, T) = G_{L12}(x, T) - G_{Mixture} \quad (3)$$

At zero Kelvin, where the entropy is zero, the free energies in the above definition become equal to formation energies. Due to the very strong relative stability of

the B2 CoAl phase, the smallest difference between the three-phase CoAl, Co<sub>3</sub>W, and Co mixture and the L<sub>12</sub> Co<sub>3</sub>(Al,W) phase at 0 K is 27 meV/atom, as shown in Figure 2a. This energy difference lowers to 22 meV/atom if the PBEsol functional is used. This minimum occurs at W rich composition.

The L<sub>12</sub> cluster expansion was fit to the 63 formation energies of Figure 2a using a genetic algorithm<sup>34</sup> and a depth first search method<sup>25</sup> to determine the optimal set of basis functions. The final basis set comprised of 25 clusters with the cluster expansion fit having a cross-validation score of 0.5 meV/atom, an error comparable in magnitude to the expected numerical convergence errors of the DFT calculations. The magnitude of the ECIs are shown in Figure 2b. The largest pair interaction connects B-sublattice sites of opposite corners of the L<sub>12</sub> cubic unit cell, having a magnitude of 13.5 meV/atom. The most closely-packed triplet and quadruplet clusters have magnitudes of 10.3 and 8.5 meV/atom, respectively. The formation energies predicted by the cluster expansion are overlaid in red on the DFT formation energies in Fig. 2a.

## B. Finite Temperature Effects

### 1. Configurational Entropy

The zero Kelvin DFT prediction that a three phase mixture of A3 Co, B2 CoAl and D0<sub>19</sub> Co<sub>3</sub>W is more stable than any configuration along the L<sub>12</sub> Co<sub>3</sub>(Al<sub>1-x</sub>W<sub>x</sub>) pseudobinary suggests that other finite temperature effects are responsible for the experimentally observed L<sub>12</sub>

crystal structure. Contributions from configurational entropy to the free energy due to Al/W mixing over the B sublattice of  $L1_2$  are a potential source of finite temperature stability. We performed semi-grand canonical Monte Carlo simulations on the cluster expansion for  $L1_2$   $\text{Co}_3(\text{Al}_{1-x}, \text{W}_x)$  to calculate a relation between the exchange chemical potential  $\tilde{\mu}_W = \mu_W - \mu_{\text{Al}}$  and B sublattice concentration  $x$ . This exchange chemical can be integrated with respect to  $x$  to obtain an expression for the Gibbs free energy,  $G_{\text{config}}$ , of  $L1_2$  according to:

$$G_{\text{config}}(x) = G_{\text{config}}(x^{\text{ref}}) + \int_{x^{\text{ref}}}^x \tilde{\mu}_W dx \quad (4)$$

where  $x^{\text{ref}}$  represents a reference W concentration on the B sublattice. The reference concentration was taken as  $x=0$  and the Gibbs free energy at that concentration,  $G_{\text{config}}(x^{\text{ref}})$ , is equal to the formation energy of the  $L1_2$   $\text{Co}_3\text{Al}$  configuration due to the absence of configurational entropy in a perfectly ordered compound.

The Gibbs free energy is plotted as a function of  $x$  at three different temperatures in Fig. 3. The effects of configurational entropy are greatest at  $\text{Co}_3\text{Al}_{0.5}\text{W}_{0.5}$  where there is equal mixing of Al and W on the B sublattice. At 0 K, the relative stability energy at this composition is 56 meV/atom. When finite temperature contributions due to configurational excitations are accounted for,  $\Delta G_{\text{stab}}$  decreases but remains positive. At 1173 K, where  $L1_2$  is experimentally observed,  $\Delta G_{\text{stab}}$  decreases to 43 meV/atom, indicating that a three phase mixture between Co, CoAl and  $\text{D0}_{19}$   $\text{Co}_3\text{W}$  is still favored in spite of the additional configurational entropy in  $L1_2$ . At concentrations  $x > 0.5$ ,  $L1_2$  becomes more competitive relative to the Co-CoAl- $\text{Co}_3\text{W}$  mixture but the stabilizing effect of configurational entropy is also less than that at  $x = 0.5$ . Compositions containing  $80 \pm 2.5$  at% W on the  $L1_2$  B sublattice remain the most competitive relative to the three-phase ground state in the 873-1473 K temperature range when configurational effects are incorporated. The most favorable composition at 1173 K is  $\text{Co}_3\text{Al}_{0.19}\text{W}_{0.81}$  with a stability free energy of  $\Delta G_{\text{stab}} = 19.6$  meV/atom. Even at temperatures approaching melting, contributions from configurational excitations are not sufficient to stabilize  $L1_2$  relative to the three-phase ground state.

## 2. Vibrational Entropy

We calculated the vibrational free energies of pure Co (both fcc and hcp), B2 CoAl, and  $\text{D0}_{19}$   $\text{Co}_3\text{W}$  within the quasi-harmonic approximation. The vibrational entropy is equal to minus the slope of the vibrational free energy with respect to temperature. The vibrational entropies of fcc Co, B2 CoAl, and  $\text{D0}_{19}$   $\text{Co}_3\text{W}$  are shown in Figure 4a. The B2 CoAl compound has the lowest vibrational entropy among the three phases. Shorter bond lengths are generally associated with stiffer bonds and therefore less vibrational entropy<sup>35</sup>. The nearest neighbor bond length

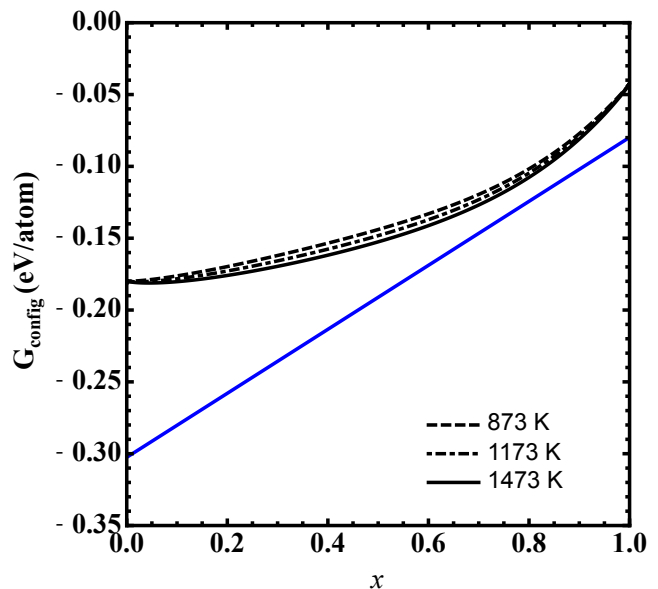


FIG. 3. Effect of configurational entropy on the  $L1_2$  structure. Black  $L1_2$  free energy curves at increasing temperature are plotted relative to the free energy of the three-phase ground state in blue.

of B2 CoAl is 2.47 Å, which is shorter than the 2.50 Å and 2.55 Å nearest neighbor bond lengths in fcc Co and  $\text{D0}_{19}$   $\text{Co}_3\text{W}$ , respectively. Strong Co-Al bonds in B2 CoAl is consistent with the very large magnitude of the B2 CoAl formation energy.

The vibrational free energies of  $L1_2$   $\text{Co}_3\text{Al}$  and  $L1_2$   $\text{Co}_3\text{W}$  were also calculated within the quasi-harmonic approximation. The vibrational entropy as a function of temperature for the two  $L1_2$  compounds is shown in Figure 4b. At 1173 K, there is an approximate 0.5  $k_B$ /atom difference in vibrational entropy between  $L1_2$   $\text{Co}_3\text{Al}$  and  $L1_2$   $\text{Co}_3\text{W}$ . The vibrational entropy of  $L1_2$   $\text{Co}_3\text{W}$  is slightly lower than that of  $L1_2$   $\text{Co}_3\text{Al}$  in spite of the heavier mass of W. This may be due to stronger bonds in the W-compound as Co-W prefers close-packed phases at the  $L1_2$  composition, while Co-Al prefers a two-phase mixture between bcc based B2 CoAl and Co at the same composition.

It is computationally prohibitive to calculate the vibrational entropy of all 63 structures along the pseudobinary line used to fit the cluster expansion for  $L1_2$ . Therefore, the vibrational free energy at intermediate compositions were modeled as a rule of mixtures between the  $\text{Co}_3\text{Al}$  and  $\text{Co}_3\text{W}$  endpoints. Configurational and vibrational entropy in the  $L1_2$  structure along the  $\text{Co}_3\text{Al}$ - $\text{Co}_3\text{W}$  pseudobinary line are plotted against each other in Fig. 5. In this plot, the vibrational entropy is measured relative to the vibrational entropy of an equivalent three-phase mixture of Co, CoAl, and  $\text{D0}_{19}$   $\text{Co}_3\text{W}$  at a given composition. It is clear that vibrational entropy is much greater in magnitude than configurational entropy across the pseudobinary, especially at the Al-rich end. It is also notable

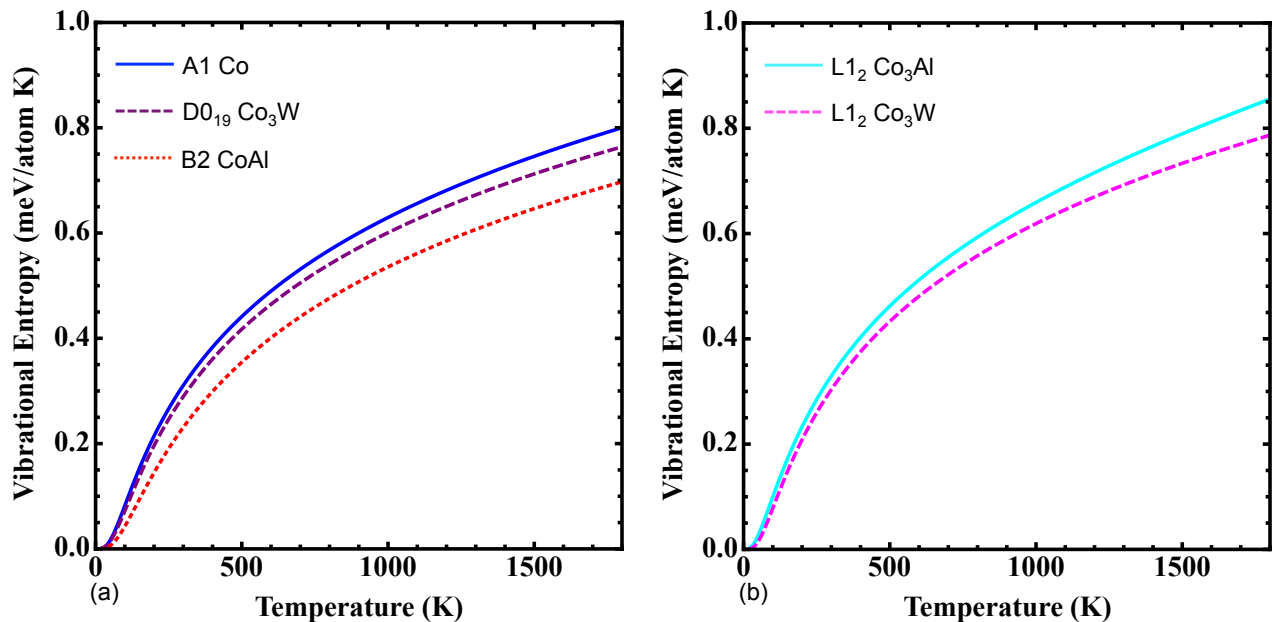


FIG. 4. Vibrational entropy as a function of temperature of the three phases comprising the ground state (a) and the  $L1_2$  endpoints of the pseudobinary (b).

that the configurational entropy is very close to the ideal entropy of mixing, suggesting that there is a nearly random solid solution of Al and W on the B sublattice in the  $L1_2$  structure.

### C. Free Energy and Stability of $L1_2$ $Co_3(Al,W)$ at Elevated Temperature

A complete expression for the Gibbs free energy of a crystal structure is approximated by summing the 0 K formation energy with the configurational and vibrational energy terms. For  $L1_2$  along the pseudobinary with B sublattice concentration  $x$ , the expression takes the following form:

$$G(x, T) = \Delta E_f + G_{config}(x, T) + G_{vib}(x, T) \quad (5)$$

An analogous free energy expression can be obtained for the three phases that make up the end points of the convex hull, but treating them as line compounds. The relative stability free energy  $\Delta G_{stab}$  of  $L1_2$  along the pseudobinary is shown in Figure 6 with increasing temperature.

At 873 K the  $L1_2$  phase becomes stable relative to the Co-CoAl-Co<sub>3</sub>W three phase mixture, with a  $\Delta G_{stab}$  of -2.2 meV/atom with 74% W on the B sublattice. The magnitude of  $\Delta G_{stab}$  increases with increasing temperature, lowering to -17 meV/atom at 1173 K. The compositions with the greatest  $L1_2$  stability at this temperature are those with approximately 70% W on the B sublattice, which is consistent with experimentally-observed compositions<sup>2</sup>. If the PBEsol functional is chosen to calculate formation energies, we find that  $\Delta G_{stab}$  will de-

crease by approximately 5 meV/atom at the most stable  $L1_2$  compositions. This choice would lower the calculated transition temperature at which  $L1_2$  becomes stable relative to the three phase mixture.

Our analysis has assumed that the three phases that

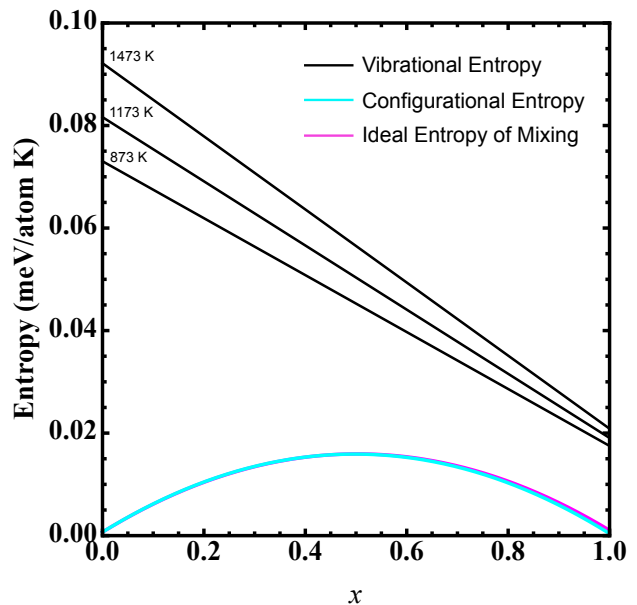


FIG. 5. The effect of configurational and vibrational entropy in the  $L1_2$  phase along the  $Co_3Al-Co_3W$  pseudobinary line. Vibrational entropy is assessed as a rule of mixtures between the two end  $L1_2$  structures relative to the vibrational entropy of an equivalent three phase mixture of A1 Co, B2 CoAl, and  $D0_{19} Co_3W$  at a given composition.



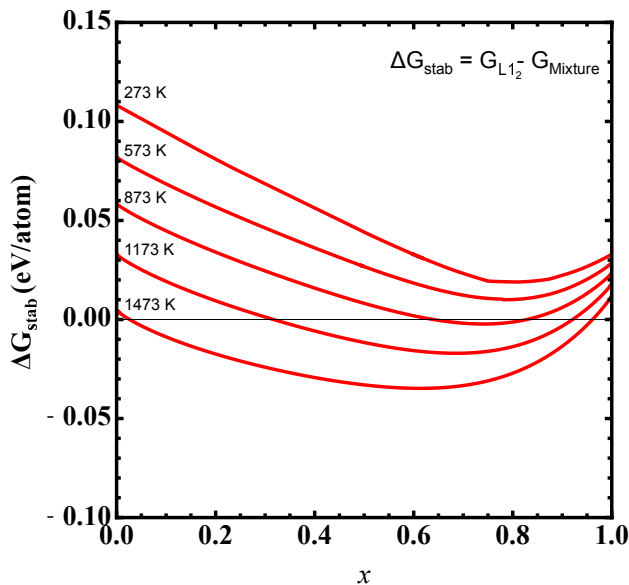


FIG. 6. Stability energy of the  $L_{12}$  structure relative to the three-phase ground state with increasing temperature.

are thermodynamically-competitive with  $L_{12}$  can be approximated as line compounds at elevated temperature. While  $D0_{19}$   $Co_3W$  does not exhibit significant solubility, B2  $CoAl$  and fcc  $Co$  have appreciable solid solubility and these effects must be accounted for in order to completely assess relative phase stability. Results from Monte Carlo simulations indicate that inclusion of configurational degrees of freedom in the free energy of B2  $CoAl$  does not appreciably change the free energy of the Al-rich end of the  $Co_3Al$ - $Co_3W$  pseudobinary. Caution should be used in drawing conclusions from the stability free energy at temperatures approaching the solvus temperature of the  $L_{12}$  phase as configurational entropy arising from an increased solubility of Al and W in fcc  $Co$  will lower its free energy and thereby reduce  $\Delta G_{stab}$  and make  $L_{12}$  less stable than predicted here. Incorporating the effects of solid solubility in elemental cobalt through a ternary cluster expansion remains a critical step in rigorously assessing phase stability in the  $Co$ - $Al$ - $W$  from first-principles.

#### IV. DISCUSSION AND CONCLUSION

We have demonstrated that  $L_{12}$   $Co_3(Al,W)$  is thermodynamically competitive relative to pure  $Co$ ,  $CoAl$ , and  $Co_3W$  at high temperature due to the combined effects of configurational and vibrational entropy. Our rigorous treatment of configurational degrees of freedom using the cluster expansion method showed that the entropy due to Al-W disorder over the B site of  $L_{12}$  at high temperature approaches that of an ideal solution. While configurational entropy is thereby maximized it is not large enough to stabilize  $L_{12}$  relative to  $Co$ ,  $CoAl$ , and  $Co_3W$ . Vibrational entropy is found to be substantially more impor-

tant in stabilizing  $L_{12}$ . Vibrational entropy is predicted to be larger in the fcc phases (fcc  $Co$  and  $L_{12}$ ) than in B2  $CoAl$  and the hcp phases (hcp  $Co$  and  $D0_{19}$   $Co_3W$ ). The very negative formation energy of B2  $CoAl$ , which favors this phase at low temperature, translates into stiff  $Co$ - $Al$  bonds. As a result, B2  $CoAl$  has the lowest vibrational entropy of all the phases considered in this work and its free energy decreases least with increasing temperature. Our study demonstrates that the inclusion of thermal expansion as modeled within the quasi-harmonic approximation is essential to render  $L_{12}$  thermodynamically stable at elevated temperature. A recent study by Saal et al<sup>18</sup>, for example, showed that vibrational free energies calculated at constant volume are insufficient to stabilize  $L_{12}$ .

The  $L_{12}$  phase that emerges at high temperature is predicted to be W rich (relative to Al). This is in large part due to the very negative formation energy of  $CoAl$  at zero Kelvin. Vibrational and configurational entropy favors slightly higher Al concentration as their inclusion causes the minimum of  $\Delta G_{stab}$  to shift to more Al rich concentrations with increasing temperature. The shift though is small and the B sublattice of  $L_{12}$  remains net rich in W at all temperature, which is consistent with experimentally-observed compositions.

In evaluating the vibrational free energy of  $L_{12}$   $Co_3(Al_{1-x}W_x)$  as a function of  $x$ , we linearly interpolated the vibrational free energies of  $L_{12}$   $Co_3Al$  and  $Co_3W$ . While an approximation, it becomes more accurate when the dependence of the vibrational free energy on the arrangement of Al and W is weak. A linear approximation should be reasonable in this system since configurational disorder in  $L_{12}$   $Co_3Al_{1-x}W_x$  occurs over the B sites, which are relatively far apart and are shielded from each other by the majority  $Co$  sublattice. This is further supported by the calculations of Saal et al<sup>18</sup> who showed that the vibrational free energy at constant volume for two different configurations at the same concentration in  $L_{12}$   $Co_3Al_{1-x}W_x$  differ only by 3 meV/atom, indicating that the vibrational free energy is relatively insensitive to the Al-W arrangement. Hence a more rigorous coupling between configurational and vibrational excitations using for example a coarse graining scheme<sup>36</sup> is not necessary.

The calculated 873 K temperature above which  $L_{12}$  is predicted to become stable is below temperatures where  $L_{12}$  is experimentally observed. Due to a variety of approximations in our treatment, we expect this predicted transition temperature to be a lower bound. Neglected in our study are the entropic contributions from configurational disorder of dissolved Al and W in fcc  $Co$ . We have also neglected entropic contributions from magnetic disorder in fcc  $Co$ . Entropy arising from spin-spiral excitations have been shown to strongly influence the hcp/fcc transition temperature for example<sup>37</sup>. The inclusion of both of these effects would stabilize elemental  $Co$  relative to the other phases and thereby increase the temperature at which  $L_{12}$   $Co_3(Al,W)$  becomes thermodynamically



cally stable.

We have shown that vibrational entropy is critical in order to thermodynamically stabilize the L1<sub>2</sub> phase in the Co-Al-W ternary. Having identified a compositional range in which this structure is most stable, it becomes evident as to how to increase the stability of L1<sub>2</sub> through further alloying. Additional components should favor L1<sub>2</sub> formation and competing phases that have a low vibrational entropy so as not to destabilize L1<sub>2</sub> at elevated temperature. It is expected that higher order alloying additions, such as Ni, Ta, and Ti, will further stabilize

L1<sub>2</sub> in Co rich alloys.

## ACKNOWLEDGMENTS

This research was supported by the National Science Foundation (NSF-DMREF-1233704). Computational resource support was provided by the Center for Scientific Computing at the CNSI and MRL: an NSF MRSEC (DMR-1121053) and NSF CNS-0960316. The authors would also like to acknowledge and thank Anirudh Natarajan and John Goiri for their assistance and useful discussions.

- 
- \* avdv@engineering.ucsb.edu
- <sup>1</sup> R. C. Reed, *The Superalloys: Fundamentals and Applications* (Cambridge University Press, 2006).
  - <sup>2</sup> J. Sato, T. Omori, K. Oikawa, I. Ohnuma, R. Kainuma, and K. Ishida, *Science* **312**, 90 (2006).
  - <sup>3</sup> T. Pollock, J. Dibbern, M. Tsunekane, J. Zhu, and A. Suzuki, *Journal of the Minerals, Metals and Materials Society* **62**, 58 (2010).
  - <sup>4</sup> S. Meher, H.-Y. Yan, S. Nag, D. Dye, and R. Banerjee, *Scripta Materialia* **67**, 850 (2012).
  - <sup>5</sup> A. Suzuki and T. M. Pollock, *Acta Materialia* **56**, 1288 (2008).
  - <sup>6</sup> M. S. Titus, A. Suzuki, and T. M. Pollock, *Scripta Materialia* **66**, 574 (2012).
  - <sup>7</sup> S. Miura, K. Ohkubo, and T. Mohri, *Materials Transactions* **48**, 2403 (2007).
  - <sup>8</sup> S. Kobayashi, Y. Tsukamoto, T. Takasugi, H. Chinen, T. Omori, K. Ishida, and S. Zaeferrer, *Intermetallics* **17**, 1085 (2009).
  - <sup>9</sup> Y. Tsukamoto, S. Kobayashi, and T. Takasugi, *Materials Science Forum* **654-656**, 448 (2010).
  - <sup>10</sup> E. Lass, M. Williams, C. Campbell, K. Moon, and U. Kattner, *Journal of Phase Equilibria and Diffusion* **35**, 711 (2014).
  - <sup>11</sup> G. Dmitrieva, V. Vasilenko, and I. Melnik, *Chem. Met. Alloys* **1**, 338 (2008).
  - <sup>12</sup> F. Xue, M. Wang, and Q. Feng, *Materials Science Forum* **686**, 388 (2011).
  - <sup>13</sup> M. Ooshima, K. Tanaka, N. L. Okamoto, K. Kishida, and H. Inui, *Journal of Alloys and Compounds* **508**, 71 (2010).
  - <sup>14</sup> A. Mottura, A. Janotti, and T. M. Pollock, *Intermetallics* **28**, 138 (2012).
  - <sup>15</sup> A. Mottura, A. Janotti, and T. M. Pollock, *Superalloys 2012*, 683 (2012).
  - <sup>16</sup> F. Xue, H. Zhou, X. Ding, M. Wang, and Q. Feng, *Materials Letters* **112**, 215 (2013).
  - <sup>17</sup> C. Jiang, *Scripta Materialia* **59**, 1075 (2008).
  - <sup>18</sup> J. E. Saal and C. Wolverton, *Acta Materialia* **61**, 2330 (2013).
  - <sup>19</sup> J. Zhu, M. Titus, and T. Pollock, *Journal of Phase Equilibria and Diffusion* **35**, 595 (2014).
  - <sup>20</sup> A. Bradley and A. Taylor, *Proc. Royal Soc* (1937).
  - <sup>21</sup> Q. Xu and A. Van der Ven, *Intermetallics* **17**, 319 (2009).
  - <sup>22</sup> J. Sanchez, F. Ducastelle, and D. Gratias, *Physica A: Statistical Mechanics and its Applications* **128**, 334 (1984).
  - <sup>23</sup> CASM, v0.1.0 (2015). Available from <https://github.com/prisms-center/CASMcode>. doi: 21 September 2015.
  - <sup>24</sup> J. C. Thomas and A. Van der Ven, *Physical Review B* **88**, 214111 (2013).
  - <sup>25</sup> B. Puchala and A. Van der Ven, *Physical Review B* **88**, 094108 (2013).
  - <sup>26</sup> A. Van der Ven, J. Thomas, Q. Xu, and J. Bhattacharya, *Mathematics and Computers in Simulation* **80**, 1393 (2010).
  - <sup>27</sup> G. Kresse and J. Furthmüller, *Computational Materials Science* **6**, 15 (1996).
  - <sup>28</sup> G. Kresse and D. Joubert, *Physical Review B* **59**, 1758 (1999).
  - <sup>29</sup> J. P. Perdew, K. Burke, and M. Ernzerhof, *Phys. Rev. Lett.* **77**, 3865 (1996).
  - <sup>30</sup> G. Kresse and J. Furthmüller, *Physical Review B* **54**, 11169 (1996).
  - <sup>31</sup> Y. Zhao and D. G. Truhlar, *The Journal of chemical physics* **128**, 184109 (2008).
  - <sup>32</sup> J. P. Perdew, A. Ruzsinszky, G. I. Csonka, O. A. Vydrov, G. E. Scuseria, L. A. Constantin, X. Zhou, and K. Burke, *Phys. Rev. Lett.* **100**, 136406 (2008).
  - <sup>33</sup> M. Born, *Dynamical theory of crystal lattices* (Oxford Univ. Press, 1966).
  - <sup>34</sup> G. Hart, V. Blum, M. Walorski, and A. Zunger, *Nature Materials* **4**, 391 (2005).
  - <sup>35</sup> A. Van De Walle and G. Ceder, *Reviews of Modern Physics* **74**, 11 (2002).
  - <sup>36</sup> G. Ceder, *Computational Materials Science* **1**, 144 (1993).
  - <sup>37</sup> M. Uhl and J. Kübler, *Physical Review Letters* **77**, 334 (1996).